Open Access

Journal of Energy and Power Technology

LIDSEN Publishing Inc.

Original Research

A Combined Power and Ejector Refrigeration Cycle System for Thermal Energy Recovery from the Waste Heat of Internal Combustion Engine

Koorosh Goudarzi *, AliReza R. Taghizadeh

Yasouj University, Yasouj 75918-74831, Iran; E-Mails: kgoudarzi@yu.ac.ir; alireza.t1075@gmail.com

* **Correspondence:** Koorosh Goudarzi; E-Mail: kgoudarzi@yu.ac.ir

Academic Editor: Islam Md Rizwanul Fattah

Journal of Energy and Power Technology
2023, volume 5, issue 1
doi:10.21926/jept.2301006

Received: December 31, 2022
Accepted: January 29, 2023
Published: February 06, 2023

Abstract

In this paper, due to the importance of energy recovery from internal combustion engines and the increasing human growing need for power and refrigeration, a two-cycle power and refrigeration system consisting of an organic Rankine cycle and an ejector refrigeration cycle is investigated analytically. The proposed system with the ability to use the ejector as an effective and economical system, can produce simultaneous power and refrigeration by drawing thermal energy from the exhaust gas and engine coolant in the form of a novel cycle. This study analyzes the proposed novel two-cycle Rankine-ejector refrigeration system (TCReRS) compared to a two-cycle Rankine-absorption refrigeration system (TCRARS). It was concluded that the TCReRS with higher output and a COP of about 69.99%, is a useful and promising system under the considered condition. The proposed system uses environmentally friendly R1233zd and R32 fluids as operating fluids in Rankine power and ejector refrigeration cycles, respectively. In addition, the effect of system performance parameters has been investigated and optimized.

Keywords

Two-cycle system; Rankine cycle; ejector refrigeration; absorption refrigeration; waste energy recovery; internal combustion engines

1. Introduction

With increasing environmental pollutants, much attention has been paid to renewable sources such as heat dissipation from internal combustion engines. Due to the cost of fuel and since a large percentage of these resources are wasted through exhaust gas and engine cooling [1], they are important sources of energy recovery and can make great progress in the future. In recent decades, the rate of patent applications in waste heat recovery technology has increased [2]. In addition to increasing efficiency, they also reduce fuel consumption [3] and help car manufacturers to control and reduce pollutants [4]. Much research has been done on energy recovery from internal combustion engines and various cycles have been used. For example, Wang et al. [5] proposed a two-cycle power generation system and R1233zd and R1234yf fluids for high-temperature and low-temperature Rankine, respectively. Another concern for human beings is their comfort, especially in indoor environments and their air conditioners. Therefore, air conditioning has been also considered in addition to generating power. On the other hand, due to environmental issues and degradation of the ozone layer, non-toxic and environmentally friendly fluids have been attracted. Both power and refrigeration generation are basic needs that can be met simultaneously with a combined power and refrigeration system. These systems are an efficient way to exploit low-cost resources [6]. There are many ways to assist in the cogeneration of power and refrigeration [7-29].

Much research has been done on the simultaneous generation of power and refrigeration, some of which have used compression refrigeration cycles. Wang et al. [30] proposed an integrated power and refrigeration system with CO_2 fluid to recover heat loss from an internal combustion engine. Other research has used the absorption refrigeration cycle [31]. Zheng et al. [32] proposed a hybrid power and refrigeration system based on the Kalina cycle. Liu and Zhang [33] proposed a new water-ammonia cycle by combining a split/adsorbent unit to generate power and refrigeration. Zhang et al. [34] also proposed several other power and refrigeration systems to produce higher energy and exergy efficiency. Wang et al. [35] proposed a power and refrigeration system combining the Rankine cycle and absorption refrigeration. Although these systems have high energy and exergy efficiency, they are relatively complex and expensive.

The ejector refrigeration system has been attractive among the refrigerant systems due to its simplicity, flexibility, high reliability, long life and low initial and maintenance costs. The ejector does not have electricity consumption or mechanical work and works at low temperatures. Thus, the ejector system seems to be a promising system for the future. A lot of research has been done using the ejector [36]. Alexis [37] introduced an ejector power and refrigeration system consisting of two Rankine and ejector refrigeration cycles. The steam-driven turbine system was used to heat the refrigerant operating fluid. Zheng and Wong [38] investigated a hybrid organic Rankine and ejector refrigeration system with R245fa operating fluid. This system had a higher refrigeration output and improved thermal efficiency. Another cycle was introduced by Dai et al. [39]. They produced power by adding a turbine between the boiler and the ejector. They also used the turbine output to launch the ejector. Wang et al. [40] studied this system under new conditions with new operating fluid. They added a pre-heater and launched the ejector with the steam-driven turbine. Their results showed that the most exergy degradation occurs in the steam generator and can be reduced by increasing the surface area and heat transfer coefficient. Wang et al. [41] proposed a hybrid power, refrigeration and heater system based on the research of Wang et al. [42]. They developed the system and used sunlight as a heat source. An extended ejector power and refrigeration system

were also investigated by Wang et al. [43] that consisted of the Brighton cycle, organic Rankine and ejector refrigeration. They also investigated the effect of thermodynamic parameters on performance and economics. In the ejector refrigeration cycle, many operating fluids, including R134a, R152a, R290, R600, R717, CO2, R11, R430A, R245fa, R600, R1234ze, R236B, and water can be used [44].

The innovation of this work is the introduction and analysis of the combined power-refrigeration cycle using the ejector to improve energy consumption. Also, the comparison of the performance of this combined cycle compared to the combined power-absorption cooling cycle that uses exhaust gases from the engine has been made for the first time. The present study proposes a two-cycle ejector power-refrigeration system to recover heat loss from internal combustion engines. The system consists of an organic Rankine cycle and an Ejector Refrigeration cycle and, unlike most previous studies, these two cycles operate separately. The heat of engine exhaust gas is used as a heat source to generate power in the Rankine cycle and then to overheat the operating fluid of the ejector refrigeration cycle. In addition to the exhaust gas heat, the Rankine cycle output heat and the heat of the engine refrigerant water are also used as heat sources in the ejector refrigeration cycle. In this study, the proposed ejector power-refrigeration cycle and a power-absorption refrigeration cycle have been analyzed to evaluate the performance and compare the outputs of these two systems. Then, the effect of the functional parameters of the system was investigated and optimized. Therefore, the main purpose of this paper is to choose a suitable combined power-refrigeration cycle for using waste energy from exhaust gases from the internal combustion engine.

2. Introducing the Proposed System and Thermodynamic Modeling

2.1 TCReRS

The proposed two-cycle Rankine-Ejector refrigeration system has been schematically illustrated in Figure 1. The bold red line indicates the engine exhaust gases at high temperature and part of its heat is captured in operator one and superheater, and then exits. The blue dotted lines represent the engine refrigerant whose heat is transferred to the cycle in evaporator 1. The pale red dotted lines represent the Rankine cycle, which comprises pump 1, recovery, evaporator 1, turbine, condenser (second cycle preheater) and reservoir. In this cycle, which operates with the R1233zd operating fluid, the fluid is pumped from the tank to evaporator one that in this path, the fluid heat is transferred to the turbine output to increase heat efficiency in the recovery part. The fluid is heated in evaporator 1, expanded in the turbine, and then transferred to the ejector refrigeration cycle in the heat condenser.

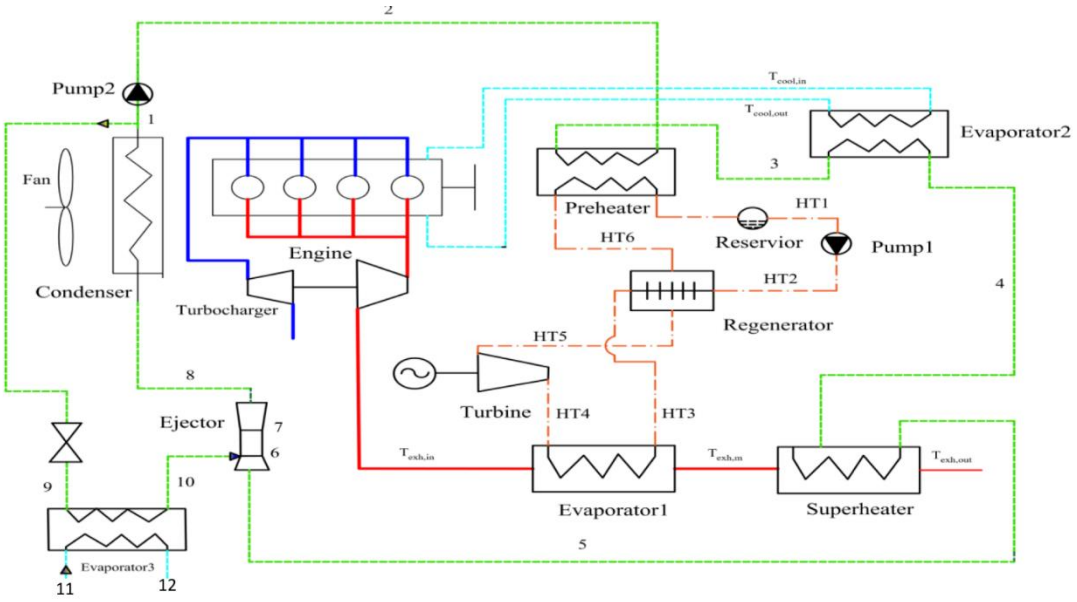

Figure 1 Two-cycle Rankine-ejector refrigeration system.

The green dotted lines represent the ejector refrigeration cycle, which includes pump 2, preheater, evaporator 2, superheater, steam ejector, condenser, pressure relief valve and evaporator 3. In this cycle, the fluid is pumped to the preheater and in the preheater; it receives the heat output of the Rankine cycle. Then, evaporator 2 receives heat from the engine refrigerant water and the superheater receives heat from the engine exhaust gas (after evaporator 1). The fluid moves to the ejector after heating and expands. The velocity of refrigerant in the ejector increases with entering into the convergent-divergent nozzle. It reaches ultrasound so that at the nozzle output, it creates a low-pressure area and results in fluid suction from the lateral inlet (evaporator 3 output). The refrigerant is then cooled in the condenser. A branch is derived from the condenser outlet to the pump that its pressure is reduced in a strangulation process; then, it receives heat from the environment in evaporator 3 and enters the ejector through the lateral inlet. In this cycle R32 is used as the operating fluid. In the kinetic energy ejector, the inlet fluid causes the lateral inlet fluid to move, so the ejector is used instead of the compressor in the refrigeration cycle. Unlike the compressor, the ejector does not require input work, which is why the ejector refrigeration cycle has a higher COP than the other refrigeration cycle. In order to verify this, an ejector refrigeration cycle is replaced by an absorption refrigeration cycle and the results of two systems of Rankine-absorption refrigeration and Rankine-Ejector are compared in this study. Evaporator 2 is assumed to be installed after the preheater and before the superheater to improve efficiency [5].

2.2 TCRARS

To compare with the power-ejector refrigeration cycle in the same system shown in Figure 1, the ejector-refrigeration cycle is replaced by the absorption-refrigeration cycle in the combined power-refrigeration cycle, which has been shown by the green lines in Figure 2 and works with the water-ammonia solution refrigerant. This cycle consists of a solution pump, heat exchanger, generator, condenser, two pressure relief valves, evaporator 3 and adsorbent. That generator, condenser, and heat exchanger operate at high cycle pressure and evaporator 3 and adsorbent operate at low pressure. In this cycle, the refrigerant also receives heat in the generator and the refrigerant steam

goes to the condenser, the engine water and the engine exhaust gas (after evaporator 1), and goes to evaporator 3 after lowering the pressure in the pressure relief valves. The concentrated solution also enters the adsorbent after passing through the heat exchanger and reducing pressure in the pressure relief valves, absorbing the solution vapor. The dilute solution obtained by the solution pump is pumped to the generator after passing through the heat exchanger and exchanging the heat with the concentrated solution. A heat exchanger has been used to increase COP in the cycle.

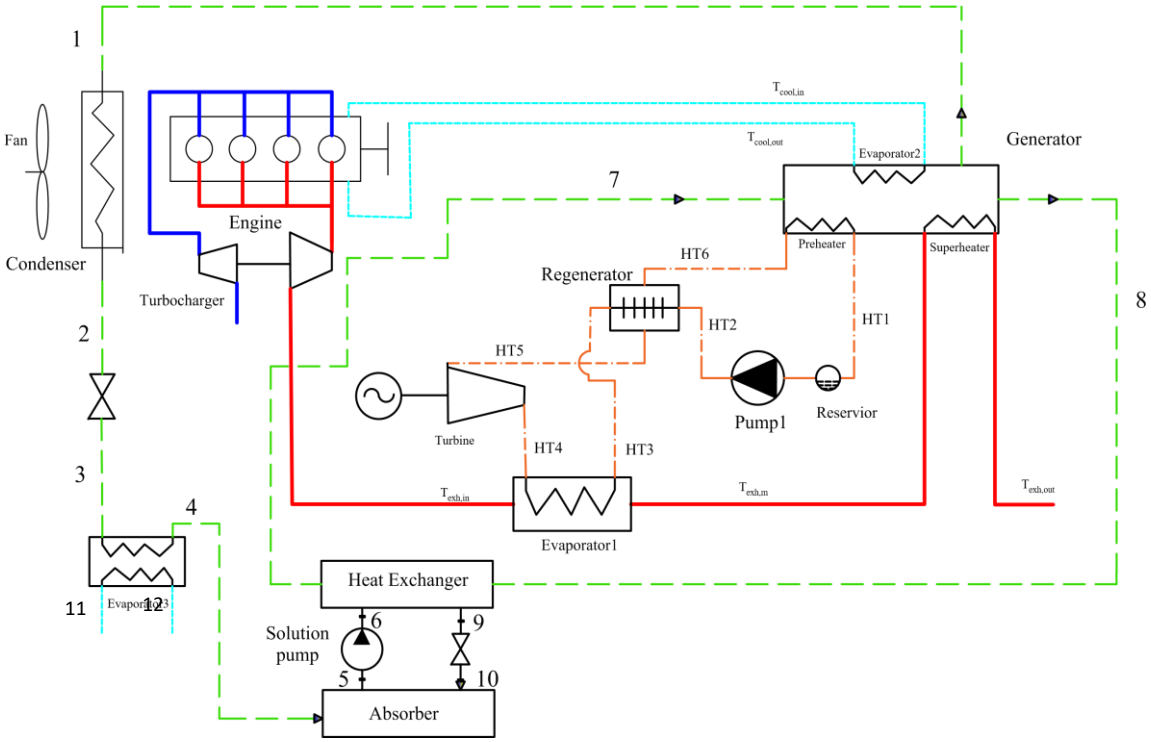

Figure 2 Two-cycle Rankine-Absorption refrigeration system.

3. Mathematical Models and Thermodynamic Analysis

3.1 Propositions

The cycles are analyzed using the relations of mass and energy conservation under stable conditions by applying the assumptions given in Table 1. This analysis was performed using engineering equation solver (EES) software with the relations of Table 1 and the input parameters listed in Table 2 and Table 3.

The following assumptions are considered in this study:

1. All processes are in a steady state.
2. Pressure drop and heat loss in pipes and processes are not considered.
3. Enthalpy remains constant for the strangulation processes in expansion valves.
4. The ejector works under ideal conditions and its performance has been considered constant.
5. The mixing process has been assumed in the constant pressure ejector.
6. The inlet of pump 1, pump 2 and the solution pump, as well as the output of the generator and evaporator 3, are saturated.
7. Kinetic energy at the input and output of the ejector has been considered negligible.

Table 1 Relationships of energy analysis in cycles.

Power generation cycle		**Refrigeration cycle**	
$P_{HT,2} = P_{HT,3} = P_{HT,4}$ and $P_{HT,1} = P_{HT,5} = P_{HT,6}$	(1)	$P_2 = P_3 = P_4 = P_5$ and $P_1 = P_8$ and $P_6 = P_7 = P_9 = P_{10}$	(14)
$h_{HT,4} = f(P_{HT,4}, T_{HT,4})$	(2)	$\dot{m}_{8.Ref} \times h_8 = \dot{m}_{5.Ref} \times h_5 + \dot{m}_{10.Ref} \times h_{10}$	(15)
$h_{HT.2} = \frac{h_{HT.2s} - h_{HT.1}}{0.8} + h_{HT.1}$	(3)	$h_5 - h_6 = \frac{{u_6}^2}{2}$	(16)
$h_{HT,5} = h_{HT,4} - (h_{HT,4} - h_{HT,5s}) \times 0.75$	(4)	$h_8 - h_7 = \frac{{u_7}^2}{2}$	(17)
$h_{HT,2} = h_{HT,3} + h_{HT,6} - h_{HT,5}$	(5)	$\omega = \frac{\dot{m}_{10.Ref}}{\dot{m}_{5.Ref}}$	(18)
$\dot{W}_{p1} = \dot{m}_{HT} \times (h_{HT,2} - h_{HT,1})$	(6)	$u_7 = \left(\frac{1}{\omega + 1}\right) \times u_6$	(19)
$\dot{W}_{t1} = \dot{m}_{HT} \times (h_{HT,4} - h_{HT,5})$	(7)	$\dot{m}_{5.Ref} \times (h_6 - h_5) = \dot{m}_{8.Ref} \times (h_7 - h_8)$	(20)
$\dot{W}_{n.TH} = \dot{W}_{t1} - \dot{W}_{p1}$	(8)	$\dot{W}_{p2} = \dot{m}_{5.Ref} \times (h_2 - h_1)$	(21)
$\dot{Q}_r = \dot{m}_{HT} \times (h_{HT,3} - h_{HT,2})$	(9)	$\dot{Q}_{B.Ref} = \dot{m}_{5.Ref} \times (h_5 - h_2)$	(22)
$\dot{Q}_{eva.1} = \dot{m}_{HT} \times (h_{HT,4} - h_{HT,3})$	(10)	$\dot{Q}_{eva,3} = \dot{m}_{10.Ref} \times (h_{10} - h_9)$	(23)
$\dot{Q}_{pre} = \dot{m}_{HT} \times (h_{HT,6} - h_{HT,1})$	(11)	$\dot{Q}_{cond} = \dot{m}_{Ref} \times (h_8 - h_1)$	(24)
$\eta_{th.HT} = \frac{h_{HT.4} - h_{HT.5} + h_{HT.1} - h_{HT.2}}{h_{HT.4} - h_{HT.3}}$	(12)	$\dot{W}_{n.comb} = \dot{W}_{n.HT} - \dot{W}_{p2}$	(25)
$\eta_{th.HT}' = \frac{h_{HT.4} - h_{HT.5} + h_{HT.1} - h_{HT.2}}{h_{HT.4} - h_{HT.2}}$	(13)	$COP = \frac{\dot{Q}_{eva,3}}{\dot{Q}_{B.Ref} + \dot{W}_{P2}}$	(26)
Ejector refrigeration system			
$Q_{u1} = Q_{u4} = 1$ and $Q_{u5} = Q_{u8} = 0$	(27)	$\dot{Q}_{E.3} = \dot{m}_{Ref,1} \times (h_4 - h_3)$	(32)
$T_9 = \varepsilon \times T_6 + (1 - \varepsilon) \times T_8$	(28)	$\dot{Q}_{cond} = \dot{m}_{Ref,1} \times (h_2 - h_1)$	(33)
$\dot{m}_{Ref.7} \times h_7 = \dot{m}_{Ref.1} \times h_1 + \dot{m}_{Ref,8} \times h_8$	(29)	$\dot{W}_{p.s.p} = \dot{m}_{Ref,7} \times (h_6 - h_5)$	(34)
$\dot{m}_{Ref.7} \times x_5 = \dot{m}_{Ref.1} \times x_1 + \dot{m}_{Ref,8} \times x_8$	(30)	$\dot{W}_{n.comb} = \dot{W}_{n.HT} - \dot{W}_{s.p}$	(35)
$h_6 = \frac{h_{6s} - h_5}{0.8} + h_5$	(31)	$COP = \frac{\dot{Q}_{eva,3}}{\dot{Q}_{G.Ref} + \dot{W}_{s.p}}$	(36)

3.2 Performance of the TCReRS

Table 2 is used to analyze the ejector refrigeration cycle. Regardless of the pressure drop, it can be said that the recovery processes, evaporator one and preheater are carried out by Equation (1) at constant pressure. Equation (2) shows that the thermodynamic properties of the HT4 point depend on the temperature and pressure of this point and that its temperature and pressure vary with the engine running at different operating conditions. The efficiency of pump one and the turbine is applied using equations (3) and (4), respectively. Equation (5) results from the energy conservation equation in the recovery. Equations (6) to (11) are used to calculate the work of pump 1, turbine work, net output work, exchange heat in recovery, the heat of evaporator 1, and preheater heat, respectively. Also, the temperature of the exhaust gas and the temperature of the engine coolant are 290 and 90°C respectively.

Table 2 Parameters of ejector-refrigeration cycle.

Parameter	Value
Inlet pressure of the turbine	4-10 MPa
Condensation temperature of the Rankine cycle	75°C
Condensation temperature of the Refrigeration Ejector cycle	15°C
PPTD of preheater	5°C
PPTD of Regenerator	5°C
PPTD of the superheater	20°C
PPTD of Evaporator 1	20°C
PPTD of Evaporator 2	5°C
PPTD of Evaporator 3	5°C
Mass flow rate of water in evaporator 3	1 kg/s
Entrainment ratio for ejector	0.7
Isentropic efficiency of Turbine	75%
Isentropic efficiency of Pumps 1 and 2	80%
Isentropic efficiency of solution pump	80%

Regarding the energy recovery relations, we use Equation (12) to calculate the thermal efficiency of the power generation cycle along with the recovery and Equation (13) to calculate the thermal efficiency of the same cycle without recovery. Equation (14), like Equation (1), expresses the isobar points in the ejector refrigeration cycle. The pressure of different areas of the ejector cycle, according to the critical points and the COP, has been set at 4.1, 0.45 and 0.1878 MPa from high to low pressure, respectively. Equation (15) represents the first law of thermodynamics in the ejector, and the first law of thermodynamics has also been written in Equations (16) and (17) according to the assumptions and regardless of the potential energy. In order to solve these Equations, Equation (19) is needed and the ratio of the mass rate of the lateral input to the main input given in Equation (18) must be calculated first.

If the energy conservation equation is written for the steam ejector's initial and end parts and then merged, Equation (20) will be obtained given that the lateral input is after point 6, and there is no heat and power exchange. Using equations (21) to (26), the work of pump 2, input heat of the cycle, heat transferred in evaporator 3, heat exchanged in the condenser, net output work of the two-circuit system, and ejector refrigeration cycle performance coefficient can be calculated.

3.3 Performance of Rankine-absorption Refrigeration System

The high and low pressures of the absorption refrigeration cycle are 15.79 and 7.211 MPa, respectively, while the generator's fraction of ammonia of output steam has been considered 1. In the absorption refrigeration cycle, it has been assumed that the generator output, evaporator three output and solution pump inlet are saturated. This has been illustrated in Equation (27). Equation (28) is also obtained from the balance of energy in the heat exchanger, where ε is the coefficient of the impact of the heat exchanger. Equation (29) is derived from the energy conservation equation in the generator. Equation (30) results from the mass conservation equation, where x is the solution mass fraction. Using Equation (31), the solution pump efficiency is applied.

The heat transferred in evaporator 3, the heat exchange in the condenser, the solution pump work, the output of the two-circuit system, and the ejector refrigeration cycle performance coefficient can be calculated using equations (32) to (36), respectively. It should be noted that due to the similarity of sources the input heat to the refrigeration cycles in the two systems, the input heat to the absorption refrigeration cycle (Q_G) is equal to Q_B in the ejector refrigeration cycle.

The parameters in Table 3 are used to analyze the absorption refrigeration cycle. For providing the same analysis conditions in the two absorption and ejector refrigeration cycles, the amount of heat input to the refrigeration cycle is assumed to be under the same engine operating conditions.

Table 3 Parameters of absorption refrigeration cycle.

Parameter	Value
Evaporator 3 temperature	278.15–288.15 K
Absorber temperature	288.15–303.15 K
Condenser temperature	283.15–288.15 K
Generator temperature	363.15 K
Mass flow rate of Generator input	1 kg/s
Rate mass of ammonia in solution in point 1	0.988
Solution heat exchanger effectiveness (Ɛ)	80%
Isentropic efficiency of Pump 2	80%

3.4 Selection of the Appropriate Working Fluid for the Ejector Refrigeration Cycle

The appropriate working fluids have been selected from the various operating fluids' properties some of which have been listed in Table 4. Based on environmental factors and improving the Rankine cycle efficiency, the R1233zd operating fluid was used in this cycle and the cycle mass rate was 0.3315 kg/s for this fluid [5]. In order to select the appropriate operating fluid for the ejector refrigeration cycle, the cycle performance has been calculated using different operating fluids and compared in Table 5.

Table 4 Properties of some of the appropriate working fluids.

Working fluid	Molecular mass (kg/kmol)	Normal boiling point (K)	Critical pressure (MPa)	Critical temperature (K)	GWP	ODP
R22	86.47	369.3	232.3	4.989	1810	0.05
R32	52.02	351.3	221.5	5.784	675	0
R41	34.03	317.3	194.8	5.897	92	0
R407c	86.2	359.3	229.5	4.632	1774	0
R410a	72.59	344.5	221.7	4.901	146	0.12

Table 5 Functional parameters in ejector refrigeration cycle.

Working fluid	$\dot{m}_p$ (kg/s)	W_{p2} (kW)	UA_{pre} (W/K)	UA_{e2} (W/K)	UA_{e3} (W/K)	UA_s (W/K)	COP
R22	1.09	2.918	1390	313	29070	931	0.6725
R32	0.516	2.867	1809	733	3924	1304	0.6999
R41	0.709	4.192	1141	2094	35400	672	0.6767
R407c	1.086	2.609	1249	293	39220	1782	0.6685
R410a	1.049	3.514	1237	319	39530	1612	0.6727

The size and cost of the heat exchanger can usually be evaluated by the UA parameter, which is the coefficient of heat transfer U from area A. The higher coefficient indicated a larger heat exchanger, and the larger size indicates a higher cost.

The UA relation is defined as follows:

$$UA = \frac{Q}{\Delta T_{lm}} \tag{37}$$

In this relation, Q is the heat transferred and ΔT_{lm} is the logarithmic temperature difference defined as follows:

$$\Delta T_{lm} = \frac{\Delta T_1 - \Delta T_2}{\ln\left(\frac{\Delta T_1}{\Delta T_2}\right)} \tag{38}$$

In this relation, ΔT_1 is the highest and ΔT_2 is the lowest temperature difference between the two ends of the heat exchanger.

R22 and R407c are not recommended among the introduced fluids due to their GWP coefficient of more than 1000 for energy recovery from internal combustion engines because they are flammable and not environmentally friendly. Table 5 presents some functional parameters calculated with different operating fluids. Among these operating fluids, R32 has the highest COP. On the other hand, this fluid is environmentally friendly and generally less expensive than other operating fluids. This fluid seems to be a good suggestion as the operating fluid of the ejector refrigeration cycle. According to the obtained results and studies, the R32 operating fluid is selected as the operating fluid for the ejector refrigeration cycle. The ammonia-water solution has also been selected as the solution pump's operating fluid of the absorption refrigeration cycle. On the other hand, to compare the turbine's performance with various operating fluids, two important indices of VFR and SP parameters are used [45].

These two parameters are defined as follows:

$$VFR = {}^{V_{out}}/_{V_{in}} \tag{39}$$

$$SP = \frac{\sqrt{V_{out}}}{\Delta h_{is}^{0.25}} \tag{40}$$

In this equation, V_{in} and V_{out} are the turbine inlet and outlet flow rates, respectively, and Δh_{is} is the isentropic enthalpy difference calculated over the turbine. VFR indicates the number of turbine parts and SP is the parameter of turbine size. The lower value of the VFR parameter means a smaller number of turbine parts so it can be said that it increases turbine efficiency. Generally, if the VFR is less than 100, high isentropic efficiency is obtained [5, 46].

4. Results and Discussion

4.1 Validation

The proposed two-circuit system in the power generation cycle segment is similar to that proposed by Wang et al. [5]. In this regard, the results of the high-temperature Rankine cycle under the same operating conditions of the two studies are compared to ensure the accuracy of the results. These results are presented in Table 6.

Table 6 Compare the present work with Wang et al. [5].

	Present work							**Wang et al. [39]**					
Working fluid	m_{HT} (kg/s)	W_{p1} (kW)	W_{t1} (kW)	VFR_{t1}	SP_{t1} (cm)	$W_{n,HT}$ (kW)	$\eta_{th.TH}$	W_{p1} (kW)	W_{t1} (kW)	VFR_{t1}	SP_{t1} (cm)	$W_{n,HT}$ (kW)	$\boldsymbol{\eta_{th.TH}}$
R1233zd	0.3315	1.955	17.138	10.88	0.8134	15.18	21.16	1.97	17.13	10.89	0.8125	15.16	21.16
R245fa	0.3352	1.854	16.38	8.931	0.7416	14.53	20.64	1.85	16.39	8.94	0.7638	14.54	20.65
Toluene	0.1658	1.514	19.26	534	2.981	17.75	21.39	1.51	19.29	537	2.164	17.78	21.42
water	0.0354	0.2703	21.53	94.6	1.235	21.26	23.45	0.27	21.56	96.5	1.172	21.29	23.45

Table 6 shows the thermal efficiency, work of pump 1, work of turbine 1, network and SP and VFR coefficients when using R1233zd, R245fa, toluene and water fluids. It is found that the results of the present study are in good agreement with the study of Wang et al. [5] which shows the accuracy of the calculations. It is worth noting that when this cycle uses water as the operating fluid, its thermal efficiency is calculated without thermal recovery because it is higher under this condition.

4.2 Rankine-absorption Refrigeration System

Earlier, the proposed ejector system is compared with an absorption refrigeration system to evaluate its value. To this end, the results of this cycle have been presented first. The maximum heat transferred to the absorption refrigeration cycle from the high-temperature Rankine cycle, the exhaust gas in the superheater and the engine refrigerant water in evaporator 3 is about 168.4 kW. These results have been calculated under conditions where the turbine inlet pressure and temperature in the Rankine power cycle are 6 MPa and 300°C, respectively.

Considering the system capacity and input parameters in the analysis of the absorption refrigeration cycle, the thermodynamic properties of each point have been calculated and shown in Table 7. Other operation parameters of this cycle have been presented in Table 8.

Table 7 Thermodynamic properties of the absorption refrigeration cycle.

state	Pressure (MPa)	Temperature (K)	Enthalpy (kJ/kg)	Entropy (kJ/kgK)	x
HT1	0.581	348.2	294.8	1.305	-
HT2	6	352.3	300.7	1.308	-
HT3	6	447.8	439.6	1.655	-
HT4	6	573.2	655.7	2.086	-
HT5	0.581	495.2	604.0	2.122	-
HT6	0.581	357.3	465.2	1.794	-
1	15.79	353.2	1425	4.558	0.988
2	15.79	278.1	15.03	0.099	0.988
3	7.211	278.3	15.03	0.1038	0.988
4	7.211	288.2	61.48	0.2678	0.988
5	7.211	293.2	-28.99	0.2649	0.8277
6	15.79	293.4	-27.99	0.2659	0.8277
7	15.79	339.4	816.5	2.866	0.8277
8	15.79	353.2	124.7	0.9877	0.5151
9	15.79	305.4	-94.07	0.3224	0.5151
10	7.211	305.5	-94.07	0.3259	0.5151
11	0.1	318.2	188.4	0.6385	-
12	0.1	310.8	157.7	0.5409	-

Table 8 Operation parameters of the absorption refrigeration cycle.

Parameter	Value
Q_G (kW)	0.3315
Q_{eva} (kW)	30.7
Q_{abs} (kW)	37.75
Q_{cond} (kW)	932.3
W_{p1} (kW)	1.97
COP	0.1811

By examining the absorption refrigeration cycle, it can be seen that the COP can increase up to 18.11% under the best operating conditions. In this case, the evaporator three outlet water temperature drops only by 7.4°C. As this analysis is purely for comparing and demonstrating the good performance of the ejector refrigeration system, it has been performed under an optimistic condition with a theoretically high yield. However, it may not be possible in practical implementation. In Table 7, the mass ratio of the solution can only be calculated for points of the absorption refrigeration cycle. In order to find the best performance, the effect of different parameters on the system's performance must be investigated. Considering the constancy of generator heat, the effect of T_{eva}, T_{abs} and T_{cond} on COP and T_{12} should be investigated. This analysis is performed while other parameters are assumed to be constant. The results of the analysis are shown in Figure 3, Figure 4 and Figure 5.

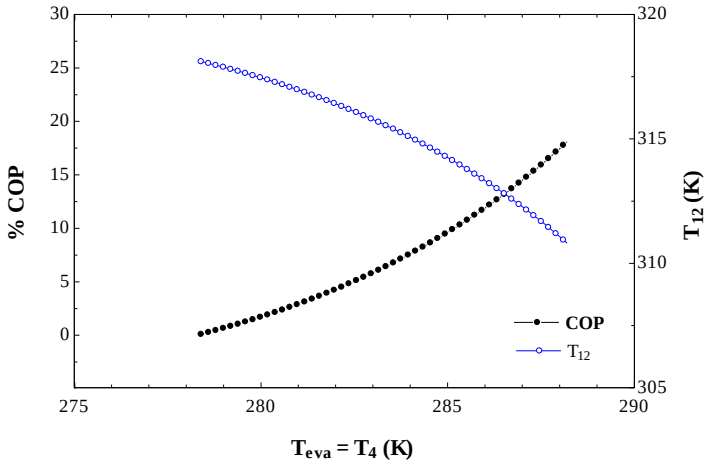

Figure 3 Influence of evaporator temperature changes on COP and outlet temperature of evaporator 3.

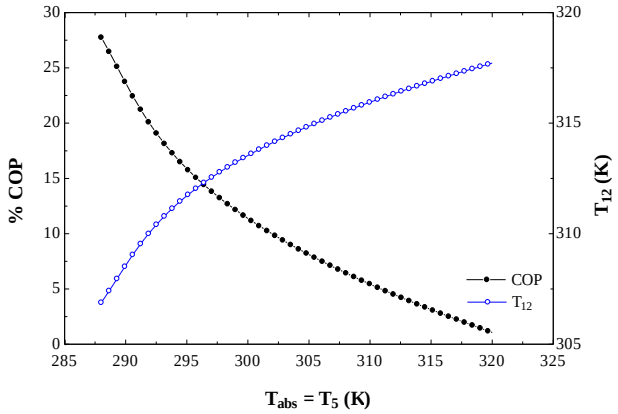

Figure 4 Influence of adsorbent temperature changes on COP and outlet temperature of the evaporator.

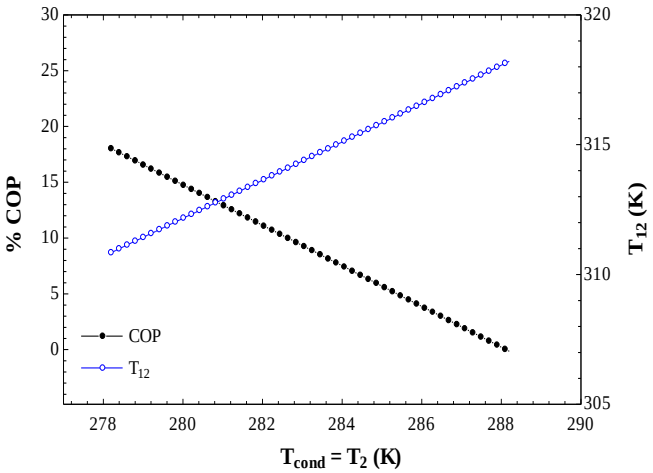

Figure 5 Influence of condenser temperature changes on COP and outlet temperature of the evaporator.

4.3 Rankine-ejector Refrigeration System

The results of this system are presented in Table 9. The maximum heat transferred to the ejector refrigeration cycle, like the absorption refrigeration cycle, is about 168.4 kW. These results have been calculated under conditions similar to the absorption refrigeration cycle where the turbine inlet pressure and temperature in the Rankine power cycle were 6 MPa and 300°C, respectively.

Table 9 Thermodynamic properties of Rankine-Ejector refrigeration cycle.

state	Pressure (MPa)	Temperature (K)	Enthalpy (kJ/kg)	Entropy (kJ/kgK)
HT1	0.581	348.2	294.8	1.305
HT2	6	352.3	300.7	1.308
HT3	6	447.8	439.6	1.655
HT4	6	573.2	655.7	2.086
HT5	0.581	495.2	604.0	2.122
HT6	0.581	357.3	465.2	1.794
1	1.281	288.2	226.8	1.094
2	5.756	291.5	232.4	1.098
3	5.756	342.4	341.9	1.442
4	5.756	347.4	360.6	1.496
5	5.756	362.4	513.3	1.929
6	0.599	264	513.3	2.189
7	0.599	264	513.2	2.189
8	1.281	288.2	513.2	2.0889
9	0.599	264	226.8	1.103
10	0.599	264	513.2	2.188
11	0.1	308.2	146.7	0.5049
12	0.1	308.2	43.23	0.155

The information shown in Table 9 has been calculated under the operating condition in which the COP reaches its maximum and the various points of the steam ejector locate in the proper operating condition. In this regard, the values of lateral ejector inlet mass flow rate ($\dot{m}_p$) and its pressure (P_{10}) have been chosen according to the diagrams shown in Figures 6a, 6b. In Figures 6a and 6b, the temperature changes of point 12 and COP have been shown versus $\dot{m}_p$ and P_{10}, respectively.

The mass flow rate passing through the pump ($\dot{m}_p$) that enters the steam ejector from the main inlet varies from 0.2334 to 0.516 kg/s and the pressure of point 10 is less than 0.599 MPa. COP remains constant at mass rates of 0.2796 kg/s to 0.339 kg/s. Another factor affecting the COP is the ratio of the mass rate of lateral input of the ejector to its main input and the condenser output temperature. Figure 6c and 6d show that with these parameters, COP increases and the outlet water temperature of evaporator 3 decreases. The range of ejector mass rate variations is less than 0.7 and the range of temperature variations of the condenser output is from 288.15 to 346 K. The COP changes versus the high pressure of the cycle are shown in Figure 6e. As expected, COP increases with increasing point pressure 3. The P3 can range from 1.291 to 5.756 MPa. In the diagram shown

in Figure 6e, the fracture is observed at a pressure of P3 = 4.538 MPa. At this pressure, point 3 is in saturation mode and the slope of the diagram is different before and after saturation pressure.

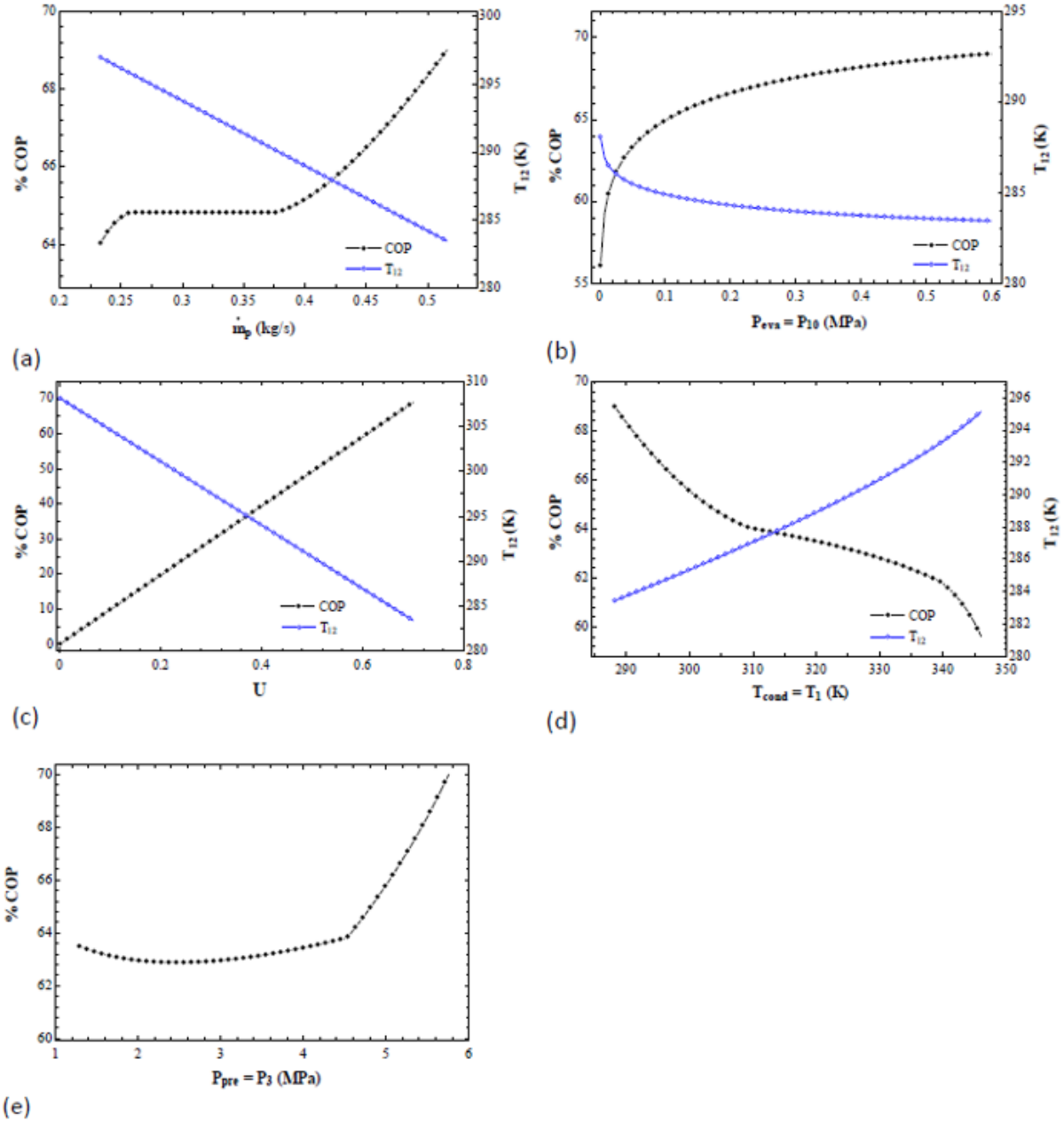

Figure 6 Influence of different parameters changes on COP and T12 (a) Ejector side inlet pressure (b) Ejector main input mass rate (c) Entrainment ratio (d) Condenser Output Temperature (e) High pressure of the system.

In this analysis, the ambient temperature is 35°C. Figure 7 shows the effect of ambient temperature changes on the outlet water temperature of evaporator 3. According to this diagram, if the temperature (is below 25°C), while the mass water rate is 1 kg/s, the water temperature of evaporator 3 will drop below 0°C and may freeze. In this regard, the problem can be solved by increasing the mass rate according to the results. Therefore, Figure 7 shows the evaporator outlet water temperature versus its inlet temperature, which is the ambient temperature, and has been

calculated at different mass rates. It can be seen that by changing the mass rate, water can be cooled without freezing.

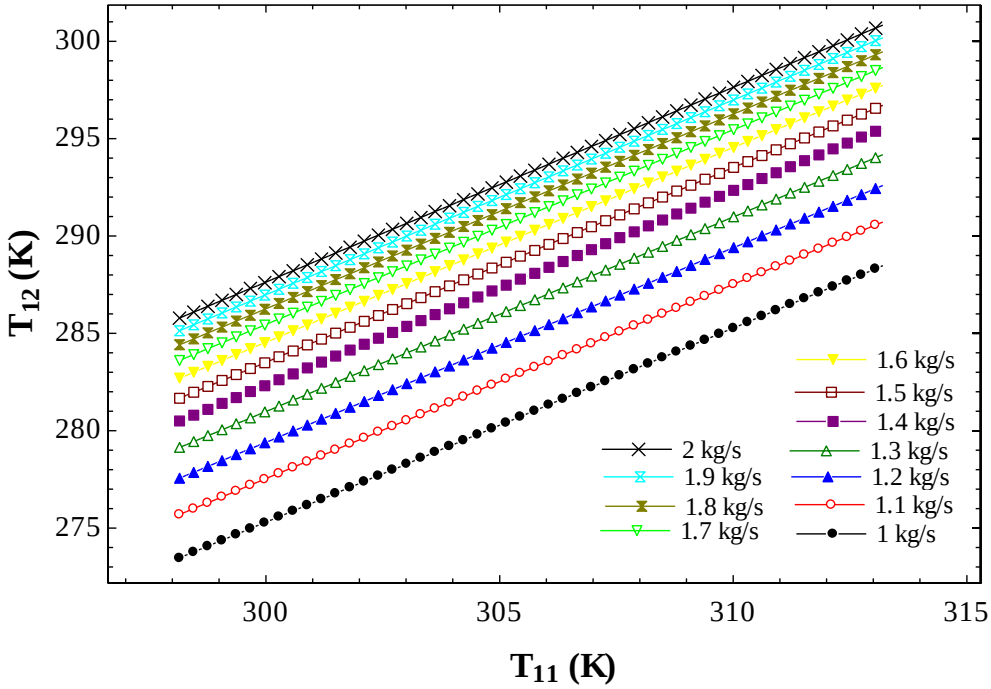

Figure 7 Influence of inlet water temperature of evaporator 3 (T11) on its outlet temperature (T12) for different mass flow rates.

Figure 8 shows the COP and T_{12} versus P10 under different conditions. Figures 8a and 8b show the effect of the system's low-pressure changes when the condenser's outlet temperature is 15, 20 and 25°C on the COP and the outlet temperature of the evaporator 3, respectively. Likewise, this analysis has been shown in Figures 8d and 8c for U values of 0.3, 0.5, and 0.7, and Figures 8f and 8e for fluid mass rates of 0.3, 0.4, and 0.5 kg/s. The results shown in Figure 8a, b show that at a constant pressure of the evaporator, the COP decreases with increasing condenser temperature. At the same time, the evaporator temperature increases with increasing condenser temperature at this pressure. Also, the results shown in Figure 8c, d indicate that the entrainment ratio greatly impacts the COP and the evaporator temperature. As the entrainment ratio increases, the COP increases by about 250% and the evaporator temperature decreases by about 95%. The effect of the mass flow rate of the pump on both of the above parameters is not very high.

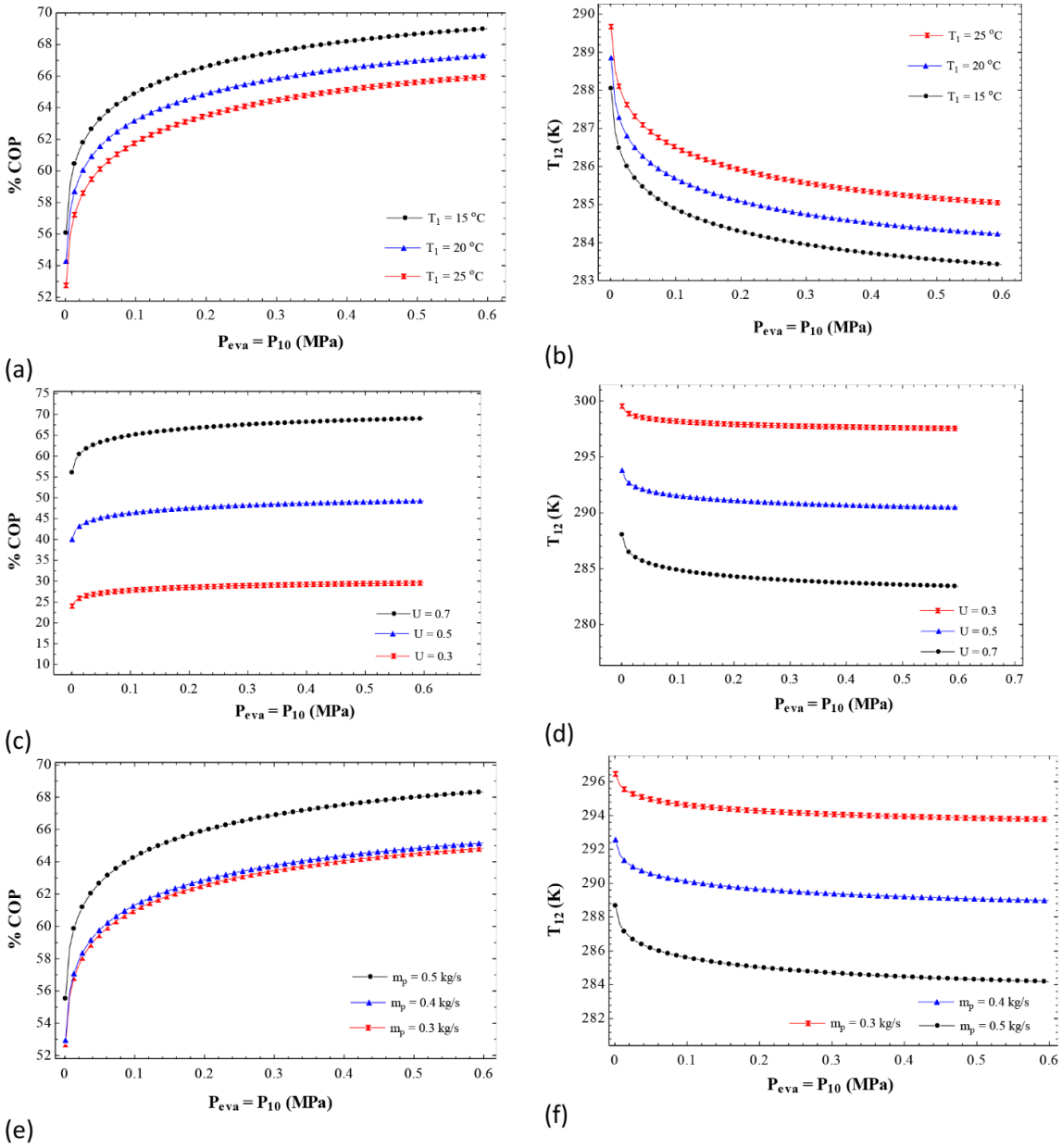

Figure 8 Influence of different parameters changes on COP and outlet water temperature of evaporator 3 (a, b) Condenser Output Temperature (c, d) Entrainment ratio (e, f) Mass flow rate of the pump.

The results show that the performance of the Rankine-ejector refrigeration system is better than the Rankine-Absorption system and its COP is about 51.88% higher. The most important reason for the high COP compared to the combined power-absorption refrigeration cycle is the use of an ejector in the combined power-ejector refrigeration cycle. Using the ejector causes the energy consumption of the cycle to decrease drastically and this causes the cycle performance coefficient to increase.

5. Conclusions

This paper analyzes the proposed novel two-cycle Rankine-ejector refrigeration system (TCReRS) compared to a two-cycle Rankine-absorption refrigeration system (TCRARS) with the first law of

thermodynamics. Results indicate that by increasing the evaporator temperature, decreasing the temperature of the absorber and the condenser temperature in the absorption refrigeration cycle as well as increasing the evaporator pressure, the flow mass rate passing through the pump, the mass flow rate in the ejector and decreasing the condenser temperature in the ejector refrigeration cycle; increase the COP and decrease the outlet temperature of the evaporator. Also, the results show that the performance of the Rankine-ejector refrigeration system is better than the Rankine-Absorption system and its COP is about 51.88% higher. Increasing the ambient temperature causes the evaporator temperature to rise, which can be compensated by lowering the water mass rate and obtaining a lower temperature for the outlet water. In the two-cycle Rankine-ejector refrigeration system, the highest COP of the ejector refrigeration cycle, about 69.99%, can be achieved.

Nomenclature

COP	Coefficient of performance	Ɛ	solution heat exchanger effectiveness
Cp	Specific heat capacity at constant pressure (kJ/kg.K)	PPTD	temperature difference
h	enthalpy(kJ/kg)	x	quality of vapor
Q	Heat transfer rate	η_{th}	Thermal efficiency
m	mass flow rate(kg/s)	GWP	global warming potential
UA	the coefficient of heat transfer	ODP	ozone depletion potential
ΔT_{lm}	the logarithmic temperature difference	ω	entrainment ration
ΔT_1	the highest temperature difference between the two ends of the heat exchanger	**subscripts**	
ΔT_2	the lowest temperature difference between the two ends of the heat exchanger	exh	exhaust gas
VFR	The number of turbine parts	In,m,out	inlet,mean,outlet
SP	the parameter of turbine size	G	generator
V_{in}	the turbine inlet flow rate	cond	condenser
V_{out}	the turbine outlet flow rate	eva	evaporator
Δh_{is}	the isentropic enthalpy difference for turbine	abs	absorption
R	gas constant	Ref	reference
P	pressure (Pa)	t	turbine
T	temperature (℃)	p	pump
W	work(J)	s.p.	solution pump
Δ	difference value	comb	combined
		cool	cooling

Author Contributions

K.Goudarzi conceived of the presented idea. K.Goudarzi and AR.Taghizadeh developed the theory and performed the computations. All authors discussed the results and contributed to the final manuscript.

Competing Interests

The authors have declared that no competing interests exist.

References

1. Domingues A, Santos H, Costa M. Analysis of vehicle exhaust waste heat recovery potential using a Rankine cycle. Energy. 2013; 49: 71-85.
2. Karvonen M, Kapoor R, Uusitalo A, Ojanen V. Technology competition in the internal combustion engine waste heat recovery: A patent landscape analysis. J Clean Prod. 2016; 112: 3735-3743.
3. Ma J, Liu L, Zhu T, Zhang T. Cascade utilization of exhaust gas and jacket water waste heat from an internal combustion engine by a single loop Organic Rankine Cycle system. Appl Therm Eng. 2016; 107: 218-226.
4. Chen T, Zhuge W, Zhang Y, Zhang L. A novel cascade organic Rankine cycle (ORC) system for waste heat recovery of truck diesel engines. Energy Convers Manag. 2017; 138: 210-223.
5. Wang E, Yu Z, Zhang H, Yang F. A regenerative supercritical-subcritical dual-loop organic Rankine cycle system for energy recovery from the waste heat of internal combustion engines. Appl Energy. 2017; 190: 574-590.
6. Kim YM, Shin DG, Kim CG, Cho GB. Single-loop organic Rankine cycles for engine waste heat recovery using both low-and high-temperature heat sources. Energy. 2016; 96: 482-494.
7. Yang MH, Yeh RH. Thermodynamic and economic performances optimization of an organic Rankine cycle system utilizing exhaust gas of a large marine diesel engine. Appl Energy. 2015; 149: 1-12.
8. Song J, Song Y, Gu CW. Thermodynamic analysis and performance optimization of an Organic Rankine Cycle (ORC) waste heat recovery system for marine diesel engines. Energy. 2015; 82: 976-985.
9. Mashadi B, Kakaee A, Horestani AJ. Low-temperature Rankine cycle to increase waste heat recovery from the internal combustion engine cooling system. Energy Convers Manag. 2019; 182: 451-460.
10. Shi L, Shu G, Tian H, Deng S. A review of modified Organic Rankine cycles (ORCs) for internal combustion engine waste heat recovery (ICE-WHR). Renew Sust Energ Rev. 2018; 92: 95-110.
11. Di Battista D, Fatigati F, Carapellucci R, Cipollone R. Inverted Brayton Cycle for waste heat recovery in reciprocating internal combustion engines. Appl Energy. 2019; 253: 113565.
12. Lu Y, Roskilly AP, Smallbone A, Yu X, Wang Y. Design and parametric study of an Organic Rankine Cycle using a scroll expander for engine waste heat recovery. Energy Procedia. 2017; 105: 1420-1425.
13. Zhu S, Deng K, Qu S. Energy and exergy analyses of a bottoming Rankine cycle for engine exhaust heat recovery. Energy. 2013; 58: 448-457.

14. Pandiyarajan V, Chinnappandian M, Raghavan V, Velraj R. Second law analysis of a diesel engine waste heat recovery with a combined sensible and latent heat storage system. Energy Policy. 2011; 39: 6011-6020.
15. Fu J, Tang Q, Liu J, Deng B, Yang J, Feng R. A combined air cycle used for IC engine supercharging based on waste heat recovery. Energy Convers Manag. 2014; 87: 86-95.
16. Wang J, Wu J, Wang H. Experimental investigation of a dual-source powered absorption chiller based on gas engine waste heat and solar thermal energy. Energy. 2015; 88: 680-689.
17. He M, Zhang X, Zeng K, Gao K. A combined thermodynamic cycle used for waste heat recovery of internal combustion engine. Energy. 2011; 36: 6821-6829.
18. Wenzhi G, Junmeng Z, Guanghua L, Qiang B, Liming F. Performance evaluation and experiment system for waste heat recovery of diesel engine. Energy. 2013; 55: 226-235.
19. Agudelo AF, García-Contreras R, Agudelo JR, Armas O. Potential for exhaust gas energy recovery in a diesel passenger car under European driving cycle. Appl Energy. 2016; 174: 201-212.
20. Dubey AM. Waste heat recovery from exhaust of diesel engines using novel organic Rankine cycle configurations: A review. J Appl Eng Res. 2018; 13: 313-316.
21. Cho H, Smith AD, Mago P. Combined cooling, heating and power: A review of performance improvement and optimization. Appl Energy. 2014; 136: 168-185.
22. Hasan AA, Goswami DY, Vijayaraghavan S. First and second law analysis of a new power and refrigeration thermodynamic cycle using a solar heat source. Sol Energy. 2002; 73: 385-393.
23. Chauhan V, Kishan PA, Gedupudi S. Thermodynamic analysis of a combined cycle for cold storage and power generation using geothermal heat source. Therm Sci Eng Prog. 2019; 11: 19-27.
24. Kazemiani-Najafabadi P, Rad EA, Simonson CJ. Designing and thermodynamic optimization of a novel combined absorption cooling and power cycle based on a water-ammonia mixture. Energy. 2022; 253: 124076.
25. Yao Y, Shi L, Tian H, Wang X, Sun X, Zhang Y, et al. Combined cooling and power cycle for engine waste heat recovery using CO_2-based mixtures. Energy. 2022; 240: 122471.
26. Anvari S, Jafarmadar S, Khalilarya S. Proposal of a combined heat and power plant hybridized with regeneration organic Rankine cycle: Energy-exergy evaluation. Energy Convers Manag. 2016; 122: 357-365.
27. Sheykhlou H, Jafarmadar S. Analysis of a combined power and ejector–refrigeration cycle based on solar energy. IJST-T Mech Eng. 2016; 40: 57-67.
28. Mansoury M, Jafarmadar S, Khalilarya S. Energy and exergy analyses of a combined cycle Kalina and organic Rankine cycles using waste heat. Int J Exergy. 2018; 27: 251-286.
29. Pashapour M, Jafarmadar S, Khalil Arya S. Exergy analysis of a novel combined system consisting of a gas turbine, an organic Rankine cycle and an absorption chiller to produce power, heat and cold. Int J Exergy. 2019; 32: 1320-1326.
30. Wang S, Bai K, Xie Y, Di J, Cheng S. Analysis of combined power and refrigeration generation using the carbon dioxide thermodynamic cycle to recover the waste heat of an internal combustion engine. Math Probl Eng. 2014; 2014: 689398.
31. Xu F, Goswami DY, Bhagwat SS. A combined power/cooling cycle. Energy. 2000; 25: 233-246.
32. Zheng D, Chen B, Qi Y, Jin H. Thermodynamic analysis of a novel absorption power/cooling combined-cycle. Appl Energy. 2006; 83: 311-323.

33. Liu M, Zhang N. Proposal and analysis of a novel ammonia–water cycle for power and refrigeration cogeneration. Energy. 2007; 32: 961-970.
34. Zhang N, Lior N. Methodology for thermal design of novel combined refrigeration/power binary fluid systems. Int J Refrig. 2007; 30: 1072-1085.
35. Wang J, Dai Y, Gao L. Parametric analysis and optimization for a combined power and refrigeration cycle. Appl Energy. 2008; 85: 1071-1085.
36. Besagni G, Mereu R, Inzoli F. Ejector refrigeration: A comprehensive review. Renew Sust Energ Rev. 2016; 53: 373-407.
37. Alexis GK. Performance parameters for the design of a combined refrigeration and electrical power cogeneration system. Int J Refrig. 2007; 30: 1097-1103.
38. Zheng B, Weng YW. A combined power and ejector refrigeration cycle for low temperature heat sources. Sol Energy. 2010; 84: 784-791.
39. Zheng B. Theoretical and experimental study on a combined power and ejector refrigeration cycle for low temperature. Shanghai, China: Shanghai Jiao Tong University; 2011.
40. Dai Y, Wang J, Gao L. Exergy analysis, parametric analysis and optimization for a novel combined power and ejector refrigeration cycle. Appl Therm Eng. 2009; 29: 1983-1990.
41. Wang J, Dai Y, Sun Z. A theoretical study on a novel combined power and ejector refrigeration cycle. Int J Refrig. 2009; 32: 1186-1194.
42. Wang J, Dai Y, Gao L, Ma S. A new combined cooling, heating and power system driven by solar energy. Renew Energ. 2009; 34: 2780-2788.
43. Wang M, Wang J, Zhao P, Dai Y. Multi-objective optimization of a combined cooling, heating and power system driven by solar energy. Energy Convers Manag. 2015; 89: 289-297.
44. Chen J, Havtun H, Palm B. Screening of working fluids for the ejector refrigeration system. Int J of Refrig. 2014; 47: 1-14.
45. Xia J, Wang J, Lou J, Zhao P, Dai Y. Thermo-economic analysis and optimization of a combined cooling and power (CCP) system for engine waste heat recovery. Energy Convers Manag. 2016; 128: 303-316.
46. Pianthong K, Seehanam W, Behnia M, Sriveerakul T, Aphornratana S. Investigation and improvement of ejector refrigeration system using computational fluid dynamics technique. Energy Convers Manag. 2007; 48: 2556-2564.